

## Studying the Structure and the Optical Properties of Pd Nanoparticles Affected by Precursor Concentration

Munaf. S. Majeed\*, Mohamed K. Dhahir\*, Zainab. F. Mahdy\*

\*(Institute of laser for postgraduate study, Baghdad University, Baghdad, Iraq

### ABSTRACT

In this paper, Palladium (Pd) nanoparticles (NPs) at different concentrations (150 and 500) capped with poly(vinylpyrrolidone) (PVP) were synthesized by a polyol reduction method in an ethylene glycol solution at a temperature of 45°C. The structural and optical properties of Pd NPs have been investigated, all thin films were tested using X-ray diffraction (XRD), all XRD peaks can be indexed as face centered cubic (FCC) structure, with strong crystalline orientation at (111) plane. The morphology properties of the prepared films were studied by Atomic Force Microscopy (AFM) the results indicated that all films have nanoscale grain size around 80 nm and Scanning Electron Microscopy (SEM) images show spherical nanoscale particles with clusters shape. The size of the particles decreased with increasing of concentrations

**Keywords** - Metallic cations, Polyol Reduction, Pd Nanoparticles, Poly (vinylpyrrolidone), Precursor concentration.

### I. INTRODUCTION

Photonics researches require materials with large nonlinear susceptibilities and fast response time. These two important properties are available in noble metal nanoparticles like gold, silver, and palladium. Such materials have close-lying bands and their conduction bands lie near Fermi level. The electrons in conduction band move nearly free with oscillation motion leads to surface resonance of the surface plasmon [1].

Among many noble metal nanoparticles, palladium occupies a large importance in hydrogen storage, sensing, and other applications which require catalytic materials [2]. In addition to catalysis and sensing, metal nanoparticles are used in optics, electronics, biomedicine cancer therapy and fuel cells that work at low temperature [3]. Noble metal nanoparticles (NPs) work as homogeneous and heterogeneous catalyst in chemical process industry, therefore; they are considered as an enhancement factor in these processes. Such properties have been of interest for centuries.

Over the last few years, efforts have been focused on manufacturing noble metal NPs with controlled size, shape, and size distribution of the nanoparticles [4]. Accordingly different methods have been employed for this purpose. One of the preferred methods over the mentioned period is polyol's synthesis. It is suitable for synthesizing noble metal nanocrystals with well-defined shapes due to the ability of polyols such as ethylene glycol (EG) to dissolve many metal salts, in addition to the dependence of the reducing power of the reaction on the temperature [5]. In this process, the EG works as

reducing agent to reduce a metallic cation to metallic colloid [6]. The reduction reaction occurs at high temperature with the assistance of polymeric stabilizer usually polyvinylpyrrolidone (PVP).

K. Patel et al. [7] synthesized Pt, Pd, Pt – Ag, and Pd – Ag nanoparticles using microwave – polyol method. In their work they studied the effect of PVP on complexing and stabilizing nanoparticles. T. Nishi et al. [8] prepared Pd nanoparticles using laser ablation in heavy and light water and tested the magnetic properties of the product.

In this paper, we report our results on preparation of well shaped Pd nanoparticles using polyol system. The effect of variation of precursor concentration on the particle size is shown. Also the experimental conditions were fixed.

### II. EXPERIMENTAL STEPS

Palladium nanoparticles (Pd NPs), prepared using Palladium nitrate dehydrate  $\text{Pd}(\text{NO}_3)_2 \cdot 2\text{H}_2\text{O}$  and Polyvinylpyrrolidone (PVP) as a stabilizer agent. They were dissolved by ethylene glycol ( $\text{C}_2\text{H}_6\text{O}_2$ ).

The samples were prepared at temperature  $(45 \pm 2)^\circ\text{C}$  for reaction time (60) min. Palladium nanoparticles (Pd NPs) were prepared by adding (500, 150) mg  $\text{Pd}(\text{NO}_3)_2 \cdot 2\text{H}_2\text{O}$  in 5 ml of ethylene glycol. Also 100 mg PVP as a stabilizing agent was dissolved in 25 ml of ethylene glycol. On the other hand 45 ml of ethylene glycol was heated by magnetic stirrer at  $(45 \pm 2)^\circ\text{C}$  for reaction time (60) minute, the temperature was monitored using a thermometer. The injection of the two solutions in the heated ethylene glycol with a burette and a syringe pump and fed to reaction mixture for 15 minute after

dosing the precursor/stabilizing agent solution. A light brown coloration was observed indicating the formation of Pd nanoparticles. After the dosing was completed, the resulting mixture was heated in the same temperature of the E.G for the same reaction time. Finally the solution was cooled to room temperature.

An optical interferometer method was used to determine the films thickness. In this method, the samples were exposed to He:Ne laser beam. An interference pattern formed due to the interference between the light beam reflected from the film surface with that reflected from the substrate. Then the sample thickness was found using the following equation [9].

$$t = \frac{\lambda \Delta x}{2x} \quad (1)$$

where  $\lambda$  is the wavelength of the laser,  $x$  is the width of the bright fringes, and  $\Delta x$  is of the dark fringes

### III. RESULTS AND DISCUSSION.

#### 3.1 Structure measurement using

##### 3.1.1 X-ray diffraction (XRD) analysis

X-ray diffraction has been employed for identification and understanding the crystalline growth nature. Diffraction patterns of the palladium nanoparticles are shown in Figs. (1) and (2) at different concentrations (150) and (500) respectively.

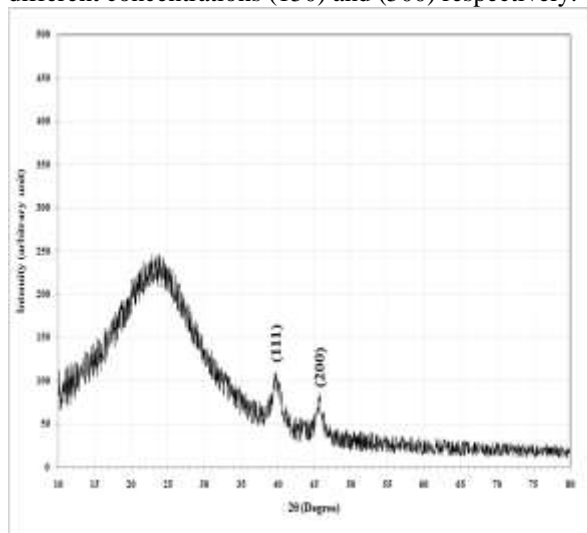


Fig.(1): The XRD pattern of Pd NPs at concentration (150).

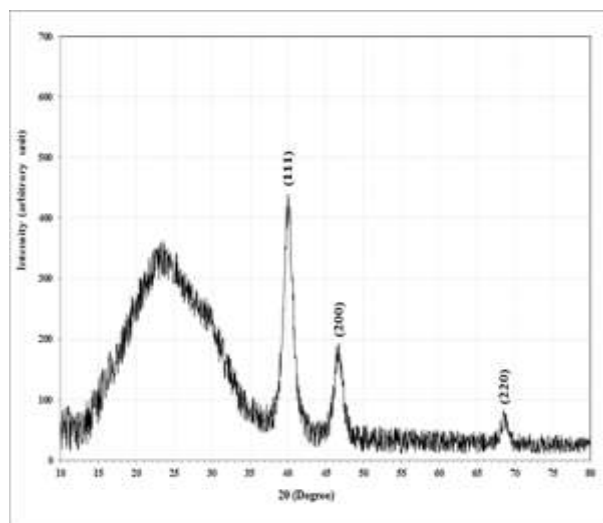


Fig.(2): The XRD pattern of Pd NPs at concentration (500).

These nanoparticles which prepared at 45C° show two different located peaks (111) and (200) for Pd (150) and three peaks from (111), (200), and (220) plans for Pd at (500) respectively. From the figures, all XRD peaks can be indexed as faced centered cubic (FCC) with strong peak at (111) direction for both concentrations. The absence of peaks of any other plans gives an indication that the product is at high purity. Further from the figure, it can be seen that the peaks' intensities increased with increased concentrations.

The grain size of the produced Pd nanoparticles can be calculated from the peak broadening using Scherer equation [10,11].

$$D = \frac{0.4\lambda}{\beta_{FWHM} \cos \theta_d} \quad (2)$$

where  $D$ : the mean diameter of the Pd nanoparticles,  $\lambda$  is the wave length of the X-ray source diffractometer, and  $\beta$  is the full-width-half-maximum (FWHM) of the XRD peak corresponding to the Bragg angle  $2\theta_d$ . Also the diffraction patterns have been used to calculate the lattice constant and the results with the grain size are listed in Tables 1 and 2 for experimental and standard values. These results show a good agreement with literature [12,13].

Table (1):- experimental and standard  $d_{hkl}$  values for Pd NPs at concentration (150)

$2\theta$ (Deg.)	FWHM (Deg.)	$d_{hkl}$ Exp.(Å)	G.S (nm)	hkl	$d_{hkl}$ Std.(Å)	Card No.
39.938	1.329	2.2556	6.4	(111)	2.2395	96-101-1106
45.714	0.954	1.9831	9.0	(200)	1.9395	96-101-1106

Table (2):- experimental and standard  $d_{hkl}$  values for Pd NPs at concentration (500).

2θ (Deg.)	FWHM (Deg.)	$d_{hkl}$ Exp.(Å)	G.S (nm)	hkl	$d_{hkl}$ Std.(Å)	Card No.
40.1188	1.4303	2.2458	5.9	(111)	2.2395	96-101-1106
46.8048	1.3437	1.9394	6.4	(200)	1.9395	96-101-1106
68.6006	1.0836	1.3669	8.9	(220)	1.3714	96-101-1106

3.1.2 AFM analysis.

The surface morphology of the Pd NPs was investigated using (AFM) analysis. The value of roughness and average grain size were calculated from the height values in AFM image using the commercial software. Fig. 3(A and B) and 4 (A and B) shows two and three-dimensional of (AFM) images of Pd NPs deposited at various construction (150, 500) respectively.

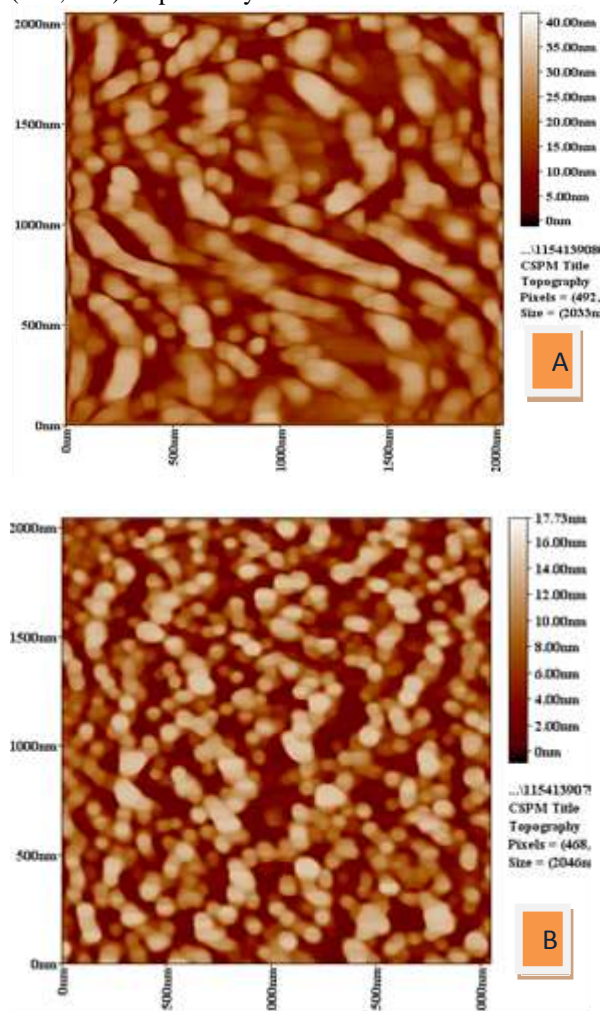


Fig. (3): Two -dimensional AFM images of Pd NPs (A 150 )and (B 500) deposited on galas plate

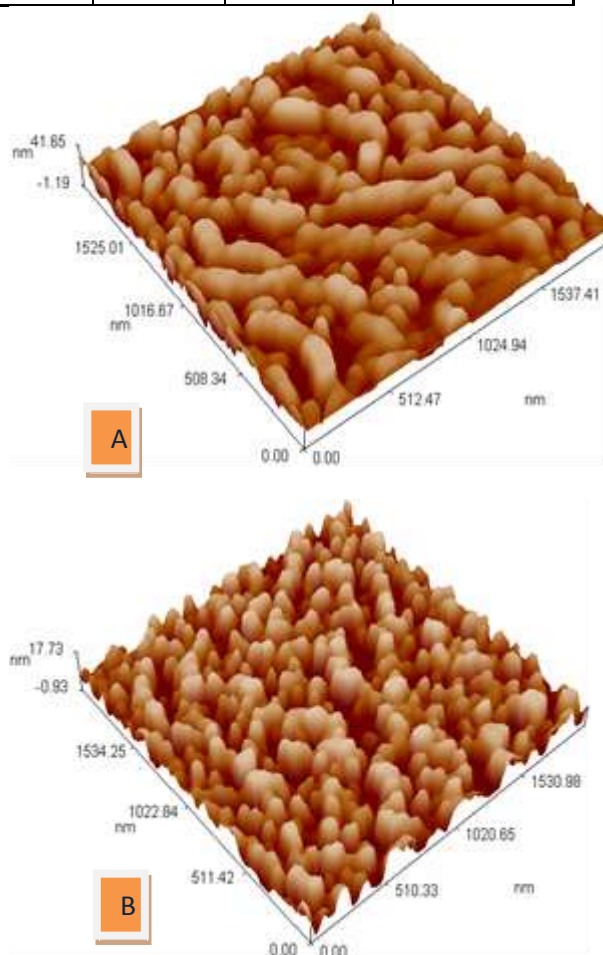


Fig. (4): Three -dimensional AFM images of Pd NPs (A 150) and (B 500) deposited on galas plate.

The average grain size of the particles is in nanoscale and the values of average grain size and surface roughness were listed in Table (3).

Table (3): Average Grain size and surface roughness of Pd NPs.

Pd at different construction	Average grain size (nm)	Roughness (nm)
150	75	6.69
500	80	3.52

A grain is a single crystalline or polycrystalline. It refers to agglomerate in bulk or thin film. The grain size is estimated by XRD pattern or Scherrer equation

but the latter is only an approximation. One particle consists of several grains and its size is larger. The particle size can be measured either by AFM, SEM, or TEM. This explanation justifies why there is a difference between nanosizes measured by AFM and that of XRD pattern. The large values given in table 3 compares to that in tables 1 and 2 indicate that our product is in polycrystalline form.

### 3.1.3 SEM Analysis.

SEM technique provides detail topography and structural information at suitable magnifications. By scanning with an electron beam, an image that is a good representation of the three dimensional sample is formed. Thus morphology studies of Pd nanoparticles were carried out with SEM and the results are displayed in Fig.(5). As seen, nanoparticles have been grown as individual clusters with a few agglomerates over the surface.

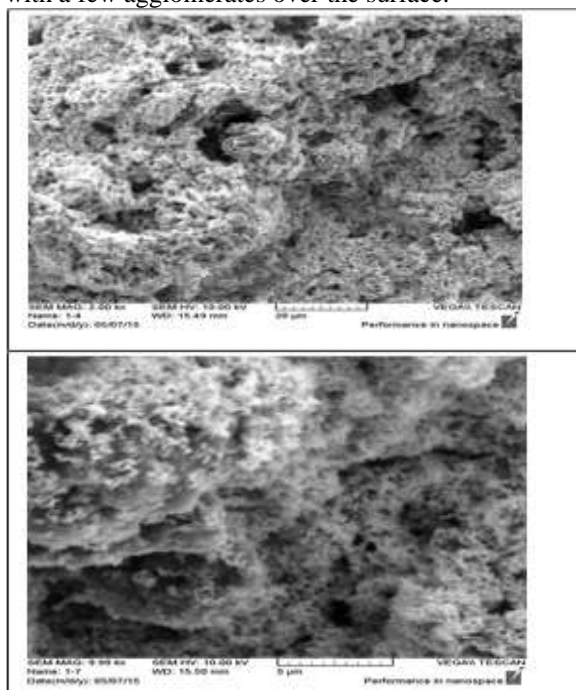


Figure 5: SEM images of Pd NPs clusters.

## 3.2 Optical measurement.

### 3.2.1 Absorbance spectrum.

UV – VIS spectrophotometer was used to record the optical absorption spectra of the Pd nanoparticles thin films. The absorption spectra for the different precursor concentration and within the wavelength range of (200 – 1100 nm) are shown in fig. 6 (A and B).

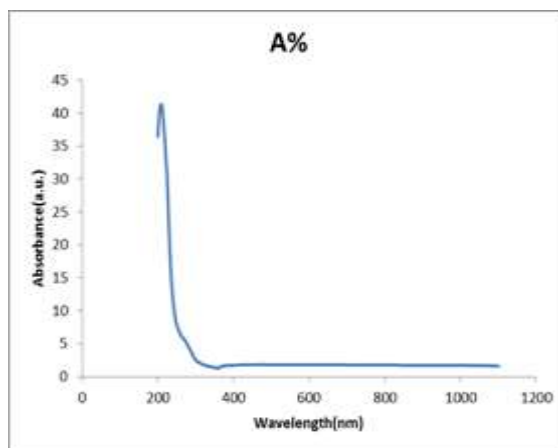


Fig.6A: Absorption spectrum of Pd NPs at construction 150.

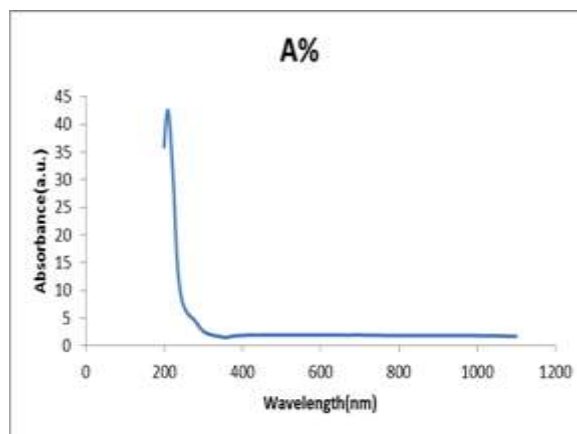


Fig.6B: Absorption spectrum of Pd NPs at construction 500.

It can be observed that when the concentration increases; the absorption value is also increases. This occurs due to the participation of more atoms in the absorption process. At visible light region, the strong photo-absorption is presented in the wavelength 330 nm at each pulse. The spectra in figure 6 (A and B) agree with references [7,14].

### 3.2.2 Absorption Coefficient and Optical Band Gap.

Materials are characterized and classified according to their optical parameters such as absorption coefficient, refractive index, and optical energy gap. These parameters can be evaluated from transmittance as well as absorbance. The absorption coefficient is obtained from the relation [15].

$$\alpha = 2.303\left(\frac{A}{t}\right) \quad (3)$$

where A is the absorbance, t = 138nm for Pd 150 and 92 nm for Pd500; is the thickness of the thin films which were obtained from Eq. (1). Both films showed decreasing in absorption coefficient with

increasing wavelength. Therefore, the samples transparency increased in the Vis – IR region. According to this result, the product can be used in solar cells.

The dependence of the optical band gap ( $E_g$ ) on the absorption coefficient and the incident photon energy ( $h\nu$ ) is given by [16].

$$(\alpha h\nu) = k(h\nu - E_g)^{\frac{1}{2}} \quad (4)$$

where  $k$  is a constant,  $\nu$  is the frequency of the incident photon. The value of  $E_g$  is obtained by plotting  $(\alpha h\nu)^2$  versus  $h\nu$  then extrapolating the linear region on the energy axis as in Fig.( 7) A and B.

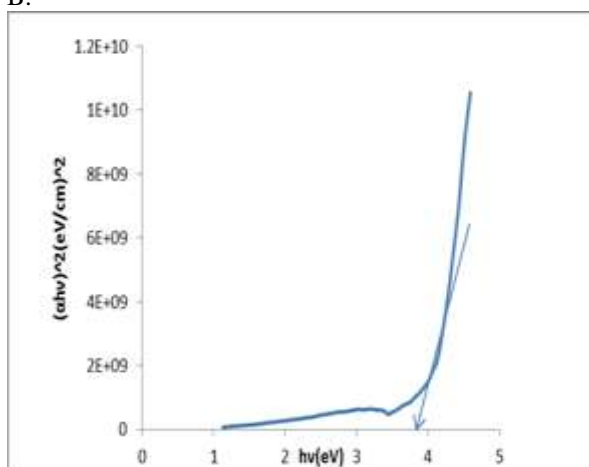


Fig. 7A: Energy gap of Pd 150.

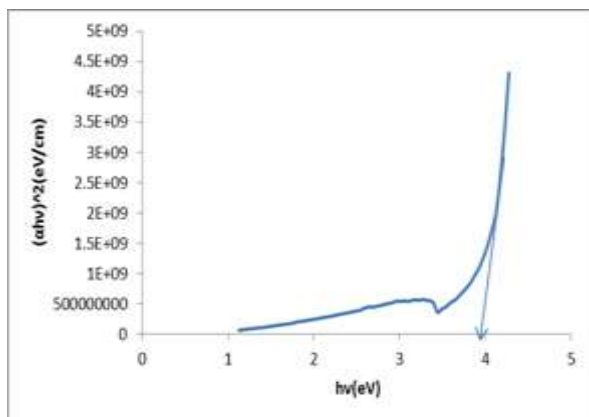


Figure 7B: Energy gap of Pd 500.

The value of  $E_g$  is 3.7 eV for 138nm film thickness and 4 eV for 92nm. The decreasing of  $E_g$  with increasing film thickness may be due to possibility of structural defects which in their rule lead to the formation of donor levels within the energy gap. These results are identical to those in reference [17].

#### IV. CONCLUSIONS

Pd nanoparticles with uniform shape were prepared by polyol method at 45°C. The current results show that polyol method is an easy and efficient method for synthesizing nanoparticles and modifying the kinetics of atoms to assembly, growth, and generate particle shapes. The size of the Pd nanoparticles could be manipulated by varying the metal precursor concentration. Further, using ethylene glycol as reducing agent leads to formation of chemical residues that can be easily removed from the reaction mixture.

#### V. Acknowledgements

This work was supported by ILPS( Institute of Laser for Post Graduate Study/ Baghdad University). We thank Dr. Abdu Alkareem, School of Since/ department of Chemistry, who conducted the AFM characterization of the samples.

#### REFERENCES

- [1] U. Gurudas, E. Brooks, D. Bubb, and et. al., Saturable and reverse saturable absorption in silver nanodots at 532 nm using picosecond laser pulses, *J. Appl. Phys. Vol. 104*, PP. 073-107, 2008.
- [2] J. Cookson, The preparation of palladium nanoparticles, *platinum metals Rev, Vol. 56, No. (2)*, PP.83-98, 2012.
- [3] H. Hei, H. He, R. Wang, and et. al., Controlled synthesis characterization of noble metal nanoparticles, *soft science letters, Vol.2*, PP.34-40, (2012).
- [4] C. Shen, C. Hui, T. Yang, and et. al. Monodisperse Noble-Metal Nanoparticles and Their Surface Enhanced Raman Scattering Properties ,*Chem. Mater. 20*, 6939–6944, 2008.
- [5] B. Lim, M. Jiang, J. Tao, and et. al. , Shape-Controlled Synthesis of Pd Nanocrystals in Aqueous Solutions, *Adv. Funct. Mater. 19*, 189–200, 2009.
- [6] D. Berger, G. Traistaru, B.Vasileand et. al., Palladium Nanoparticl Synthesis with Controlled Morphology Obtained by Polyol Method, *U.P.B. Sci. Bull., Series B, Vol. 72*, Iss. 1, 2010.
- [7] K. Patel, S. Kapoor, D. Purshot, and et. al. , Synthesis of Pt, Pd, Pt/Ag and Pd/Ag nanoparticles by microwave-polyol method, *J. Chem. Sci., Vol. 117, No. 4*, pp. 311–316. 2005.
- [8] T. Nishi, A. Takeichi, H. Azuma, Fabrication of Palladium Nanoparticles by Laser Ablation in Liquid, *JLMN-Journal of Laser Micro/Nanoengineering Vol. 5, No. 3*, 2010.

- [9] M. Hernández, A. Juárez,\* R. Hernández, Interferometric thickness determination of thin metallic films, *Superficies y Vacío* 9, 283-285, 1999.
- [10] R. Devi, P. Purka, P. Kalita, and et. al., Synthesis of nanocrystalline CdS thin films in PVA matrix, *Bull. Mater. Sci., Vol. 30, No. 2*, pp. 123–128, 2007.
- [11] I.Rathinamala, J.Pandiarajan, N. Jeyakumaran, and et. al., Synthesis and Physical Properties of nanocrystalline CdS Thin Films – Influence of sol Aging Time & Annealing Temperature, *Int. J. Thin Film Sci. Tec. 3, No. 3*, 113-120 ,2014.
- [12] V. Nguyen, D. Nguyen, H. Hirata, and et. al., Chemical synthesis and characterization of palladium nanoparticles, *Adv. Nat. Sci.: Nanosci. Nanotechnol. 1 035012* (5pp), 2010.
- [13] S. Navaladian , B. Viswanathan ,T. K. Varadarajan, and et. al., A Rapid Synthesis of Oriented Palladium Nanoparticles by UV Irradiation, *Nanoscale Res Lett* 4:181–186, 2009.
- [14] H. Hei, H. He, R. Wang, and et. al., Controlled Synthesis and Characterization of Noble Metal Nanoparticles, *Soft Nanoscience Letters*, 2, 34-40, 2012.
- [15] J. Mohammad, and H.Al-jumaili, Structural and optical properties of Nanocrystalline ZnxCd1-xS thin films deposited by chemical bath technique , *IJAEM, Volume 3, Issue 5*, 2014.
- [16] M. Baykula , A. Balcioglu, AFM and SEM studies of CdS thin films produced by an ultrasonic spray pyrolysis method, *Microelectronic Engineering 51–52* ,703–713, 2000.
- [17] F. Samavat, F. Mahmoodi, P. Ahmad, Effect of Annealing Temperature on the Optical Properties of Palladium Thin Film, *Open Journal of Physical Chemistry*, 2, 103-106, 2012.